Environmental Pollution 234 (2018) 429–438

Contents lists available at ScienceDirect

Environmental Pollution

journal homepage: www.elsevier.com/locate/envpol

Impacts of sea-land and mountain-valley circulations on the air pollution in Beijing-Tianjin-Hebei (BTH): A case study☆

Naifang Bei [a, b], Linna Zhao [c], Jiarui Wu [b], Xia Li [b], Tian Feng [b], Guohui Li [b, *]

[a] School of Human Settlements and Civil Engineering, Xi'an Jiaotong University, Xi'an, China
[b] Key Laboratory of Aerosol Chemistry and Physics, SKLLQG, Institute of Earth Environment, Chinese Academy of Sciences, Xi'an, China
[c] State Key Laboratory of Severe Weather, Chinese Academy of Meteorological Sciences, Beijing, China

ARTICLE INFO

Article history:
Received 2 March 2017
Received in revised form
16 November 2017
Accepted 20 November 2017
Available online 5 December 2017

Keywords:
Breeze
$PM_{2.5}$
Ozone

ABSTRACT

In the study, observational data analyses and the WRF-CHEM model simulations are used to investigate the role of sea-land and mountain-valley breeze circulations in a severe air pollution event occurred in Beijing-Tianjin-Hebei (BTH) during August 9–10, 2013. Both the wind observations and the model simulations have clearly indicated the evolution of the sea-land and mountain-valley breeze circulations during the event. The WRF-CHEM model generally reproduces the local meteorological circulations and also performs well in simulating temporal variations and spatial distributions of fine particulate matters ($PM_{2.5}$) and ozone (O_3) concentrations compared to observations in BTH. The model results have shown that the offshore land breeze transports the pollutants formed in Shandong province to the Bohai Gulf in the morning, causing the formation of high O_3 and $PM_{2.5}$ concentrations over the gulf. The onshore sea breeze not only causes the formation of a convergence zone to induce upward movement, mitigating the surface pollution to some degree, also recirculates the pollutants over the gulf to deteriorate the air quality in the coastal area. The upward valley breeze brings the pollutants in the urban area of Beijing to the mountain area in the afternoon, and the downward mountain breeze transports the pollutants back during nighttime. The intensity of the mountain-valley breeze circulation is weak compared to the land-sea breeze circulation in BTH. It is worth noting that the local circulations play an important role when the large-scale meteorological conditions are relatively weak.

1. Introduction

Since atmospheric pollutants have deleterious impacts on human health and the environment (e.g., Pope and Dockery, 2006; Tie et al., 2009; Zhang et al., 2010a), air pollutions has become a serious concern of the public in China along with the rapid industrialization and urbanization during recent 30 years (e.g., Chan and Yao, 2008; Fang et al., 2009). Beijing-Tianjin-Hebei (BTH) is one of the most severely polluted areas in China, characterized by high levels of fine particulate matters ($PM_{2.5}$), sulfur dioxide (SO_2), and recently increasing concentrations of ozone (O_3) (e.g., Chan and Yao, 2008; Wang et al., 2011; Feng et al., 2016; Wu et al., 2017; Li et al., 2017a, b).

The high-pollution episodes are usually consequences of strong local emissions coupled with specific meteorological conditions. When the emissions of pollutants remain invariable, the pollution situations are mainly determined by the meteorological situations and atmospheric physical and chemical processes (e.g., Bei et al., 2008, 2010; Zhang et al., 2012). For example, Tie et al. (2015) have clearly shown that the meteorological situations play an important role in the aerosol pollution in BTH. The pollution situation is generally influenced by both large-scale and local meteorological conditions. The large-scale synoptic pattern generally steers the transport and dispersion of pollutants, providing favorable conditions for pollutants accumulation (e.g., Chan et al., 1998; Wang et al., 1998; Chen et al., 2008; Zhang et al., 2012; Bei et al., 2013, 2016a, 2016b). Although local meteorological conditions are not continuously consistent with those at large scales, but still have substantial impact on the air pollution events. Particularly when the large-scale winds are weak, local circulations, such as land-sea breeze or mountain-valley breeze, can become the predominant factor in controlling the pollution situation (e.g., Liu and Chan, 2002; Ding et al., 2004; Banta et al., 2005; Bao et al., 2005; Fan

☆ This paper has been recommended for acceptance by Eddy Y. Zeng.
* Corresponding author.
E-mail address: ligh@ieecas.cn (G. Li).

https://doi.org/10.1016/j.envpol.2017.11.066
0269-7491/

et al., 2006; Zhang et al., 2007). In addition, the impact of mountains on meteorological fields has also been found to contribute substantially to the air pollution in the Guanzhong Basin (Zhao et al., 2015) and BTH (Long et al., 2016).

Great efforts have been made to explore the role of meteorological conditions and emission reductions in the air quality improvements in Beijing during the 29th Summer Olympic Games in 2008. During the 2008 Olympics period, Beijing government has implemented aggressive control strategies to decrease pollutants emissions (Parrish and Zhu, 2009), providing favorable circumstance for improvement of the air quality in Beijing. Wang et al. (2009) have found that the decreased O_3 concentration at a Beijing rural site during the 2008 Olympics period is caused by the favorable meteorological condition compared to the same period in 2006 and 2007. Zhang et al. (2009) and Wang et al. (2010) have both shown that the favorable weather conditions (such as prolonged rainfall and decreased temperature) play a key role in decreasing the level of pollutants during the 2008 Olympics period. Zhang et al. (2010b) have clarified that the atmospheric visibility improvements during the 2008 Olympics period are mostly caused by the decrease of the atmospheric relative humidity compared to the same period in the previous 5 years. Gao et al. (2011) have further verified that meteorological conditions are as important as emission mitigations in reducing $PM_{2.5}$ concentrations in Beijing during the 2008 Olympics period using a coupled meteorology-chemistry model. Zhang et al. (2012) have investigated the connection between the surface circulation pattern and the air quality in BTH using an objective classification procedure (Philipp et al., 2010). Synoptic-scale circulations have been shown to be the main drivers of day-to-day variations in pollutant concentrations over BTH, with critical differences in the local meteorology and footprints of 48-h backward trajectories among various circulation types during the emission control period (Zhang et al., 2012).

Local meteorological conditions in BTH involve interactions between sea-land and mountain-valley breeze circulations, which are driven by the local temperature contrast and the large-scale flows. Miao et al. (2015) have emphasized that the intensity of the land-sea and mountain-valley breeze circulations play an important role in the vertical transport and distribution of pollutants in BTH. The impact of the sea-land breeze circulation on pollution episodes has also been examined in coastal areas, such as Houston, Hong Kong, and the Pearl River Delta of China (e.g., Banta et al., 2005; Zhang et al., 2007; Liu and Chan, 2002; Ding et al., 2004).

In the present study, the contributions of local circulations (including sea-land breeze and mountain-valley breeze) to a heavy air pollution event occurred in BTH are investigated using the observational analyses and numerical simulations with a coupled meteorology-chemistry model. The data, model, and methodology used in this study are introduced in Section 2. The analyses on synoptic and local meteorological conditions during the episode and model simulations are shown in Section 3. Section 4 includes summary and discussions.

2. Data and model configurations

A three-day episode from 9 to 11 August 2013 is selected in the study, representing a heavy air pollution event in BTH with high levels of O_3 and $PM_{2.5}$ concentrations. The observed daily average $PM_{2.5}$ concentration in BTH is 102.4 μg m^{-3} during the episode, and the average O_3 concentration in the afternoon is 161.6 μg m^{-3}. The National Centers for Environmental Prediction (NCEP) final operational global gridded analysis (FNL) (1° × 1°) has been used to analyze the large-scale synoptic meteorological conditions over BTH during the episode. The surface hourly automatic observations in BTH have been used to demonstrate the evolutions of mountain-valley and sea-land breeze circulations. Observations from two radar wind profilers in BTH have also been employed to verify the mountain-valley and sea-land breeze circulations in the vertical direction (Fig. 1b). Since January 2013, the China's Ministry of Environmental Protection (China MEP) has commenced to release the real-time hourly concentrations of O_3 and $PM_{2.5}$ at 79 monitoring sites in 13 cities of BTH, which are used to validate the model results during the episode.

The WRF-CHEM model has been applied to further simulate the three-day severe air pollution episode in BTH. A specific version of the WRF-CHEM model, based on the previous studies (Grell et al., 2005; Fast et al., 2006), is utilized in the study, which is developed by Li et al. (2010). Further model description can be found in Supplementary Information (SI). Detailed model configurations are given in Table 1.

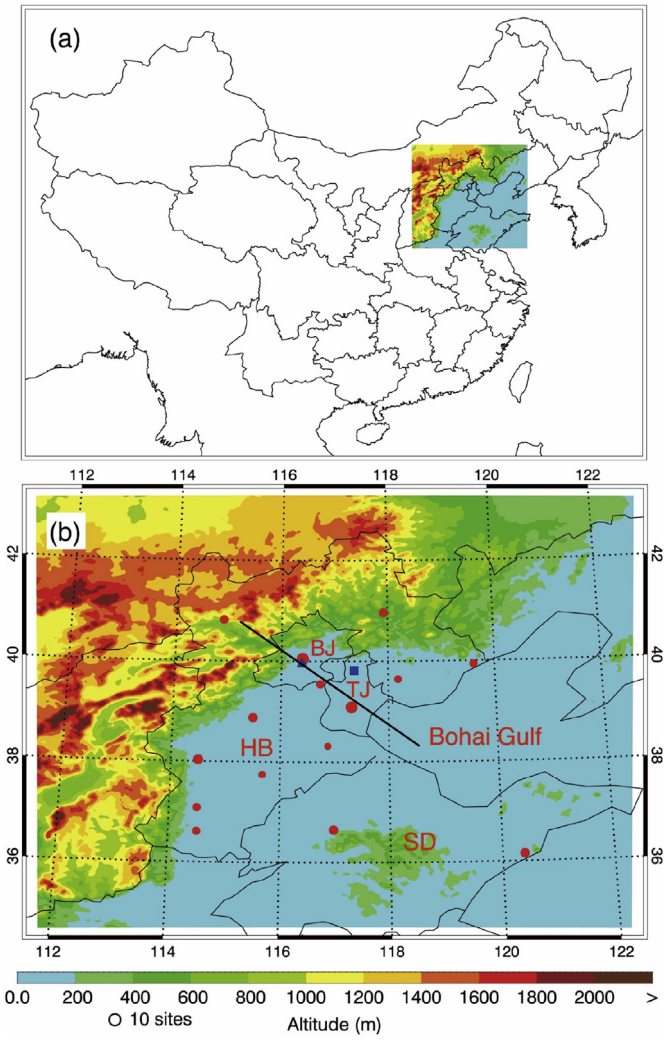

Fig. 1. (a) Map showing the location of Beijing-Tianjin-Hebei-Shandong in China and (b) WRF-CHEM model simulation domain with topography. In (b), the red filled circles represent centers of cities with ambient monitoring sites and the size of the circle denotes the number of ambient monitoring sites of cities. The blue filled triangle and square are the observation sites with wind profilers at Haidian in Beijing and at Baodi in Tianjin, respectively. The black cross line is the position of the cross-section shown in Fig. 7. BJ: Beijing, TJ: Tianjin, HB: Hebei, and SD: Shandong. (For interpretation of the references to colour in this figure legend, the reader is referred to the web version of this article.)

Table 1
WRF-CHEM model configurations.

Simulation Regions	Beijing-Tianjin-Hebei-Shandong
Simulation period	August 9 to 11, 2013
Domain size	300 × 300
Domain center	39°N, 117°E
Horizontal resolution	3 km × 3 km
Vertical resolution	35 vertical levels with a stretched vertical grid with spacing ranging from 30 m near the surface, to 500 m at 2.5 km and 1 km above 14 km
Microphysics scheme	WSM 6-class graupel scheme (Hong and Lim, 2006)
Cumulus scheme	Grell-Devenyi ensemble scheme (Grell and Devenyi, 2002)
Boundary layer scheme	MYJ TKE scheme (Janjić, 2002)
Surface layer scheme	MYJ surface scheme (Janjić, 2002)
Land-surface scheme	Unified Noah land-surface model (Chen and Dudhia, 2001)
Longwave radiation scheme	Goddard longwave scheme (Chou and Suarez, 2001)
Shortwave radiation scheme	Goddard shortwave scheme (Chou and Suarez, 1999)
Meteorological boundary and initial conditions	NCEP 1° × 1° reanalysis data
Chemical initial and boundary conditions	MOZART 6-h output (Horowitz et al., 2003)
Anthropogenic emission inventory	SAPRC-99 chemical mechanism emissions (Zhang et al., 2009)
Biogenic emission inventory	MEGAN model developed by Guenther et al. (2006)
Model spin-up time	28 h

3. Results and discussions

3.1. Synoptic meteorological conditions and the observed local circulations

Using the NCEP-FNL reanalysis data (1° × 1°), the large-scale meteorological conditions are analyzed at the surface, 850 hPa, and 500 hPa over BTH during the period from 9 to 11 August 2013. At the surface, BTH is situated at the northeast of a high pressure center, with the prevailing south wind (Figure not shown). At 850 hPa, BTH is located at a transition zone between the subtropical high in the southeast and a low in the northeast (Figs. S1a and S1b), indicating that this area is under the control of the relatively weak northwesterly flow on August 9 and southwesterly flow on August 10. The synoptic situations at 500 hPa during the two days are similar to those at 850 hPa, with a weak westerly flow over BTH (Figs. S1d and S1e). Besides, from August 9 to 10, the low located at the northeast of BTH over 850 hPa moves toward the east, with the decreasing intensity. While the high located at the south at 850 hPa moves toward the northwest, with the increasing intensity. The above analysis shows the relatively weak large-scale flow characteristics at the upper level over BTH on these two days, which are favorable for the development of the local circulations. On August 11 (Figs. S1c and S1f), BTH is located at the front of a trough both at 850 hPa and 500 hPa, with the consistent southerly wind, indicating the intensification of the air exchange between the low and high latitude regions and further facilitating the dispersion of air pollutants. Therefore, the local circulations occurred on August 9 and 10 are emphasized in the following discussions.

Fig. S2 presents the observed and calculated surface winds in BTH every 3 h on August 09, 2013. In general, the WRF-CHEM model performs reasonably well in simulating the surface winds compared to observations. The evolution of the sea-land breeze circulation is clearly exhibited along the Bohai Gulf. From the mid-night to early morning (Fig. S2a-c, 00:00–06:00 BJT), the westerly offshore flow is evident along the Bohai Gulf. From 06:00 to 09:00 BJT, the westerly offshore flow tends to decrease. Until the noon (12:00 BJT), the onshore southeasterly wind commences to appear along the coastline (Fig. S2e). From the noon to the late night (Fig. S2e-h, 12:00–21:00 BJT), the southeasterly onshore flow is prevailing along Bohai Gulf. To the mid-night (Fig. S3a, 00:00 BJT), the westerly offshore occurs near the coastline again. However, in overall, the observed and simulated sea-land breeze circulation is relatively weak on August 9. From the mid-night to the early morning on August 10 (Figs. S3a and S3b), the westerly offshore flow becomes dominant along the Bohai Gulf and gradually decays from 06:00 to 09:00 BJT (Figs. S3c and S3d). In the afternoon (Fig. S3e-g, 12:00–18:00 BJT), the onshore southeasterly wind starts to develop and become prevailing along the coastline. In the evening (Fig. S3g and S3h, 18:00–21:00 BJT), the onshore sea breeze further intrudes the land and eventually impacts Beijing (Fig. S3h). The sea-land breeze circulations on August 9 and 10 are generally similar, but the sea-land breeze circulation on August 10 is intensified compared to that on August 9. Fig. 2 shows the simulated and observed wind hodographs at two surface sites along the coastline of the Bohai Gulf on August 10, 2013. The WRF-CHEM model reasonably simulates the observed diurnal cycle at the two sites, but the simulated winds are stronger and smoother than the observations. The overestimation of the sea breeze by the model might be caused by the bias in the PBL parameterization (Zhang et al., 2007).

In addition, the mountain-valley circulations are also evident in Beijing. For example, from 00:00 to 09:00 BJT on August 9 (Figs. S2a–d), Beijing is influenced by relatively strong westerly wind down from Taihang Mountains and northerly wind down from Yanshan Mountains (mountain breeze). After 09:00 BJT, the mountain breeze starts to decrease while the valley breeze (southerly or easterly wind) increases with the maximum occurring around 15:00 BJT. Then, the southerly wind gradually decreases and the mountain breeze (westerly or northerly wind) dominates again in Beijing. The mountain-valley breeze on August 10 is relatively weak compared to that on August 9.

The mountain-valley breeze circulation has also been clearly observed by the evolution of the vertical profiles of the hourly horizontal winds provided by the radar wind profiler at Haidian in Beijing on August 9 and 10 (Fig. 3a and b). Strong wind shift has occurred around the time of 10:00–12:00 BJT on August 9 and 11:00–13:00 BJT on August 10. On August 9, the dominant wind at Haidian is northerly wind before 10:00 BJT and turns into southerly wind after 11:00 BJT. On August 10, the prevailing wind is northeasterly before 12:00 BJT and shifts to southerly wind after 12:00 BJT. Additionally, the wind speed around the transition time (11:00–13:00 BJT) is substantially decreased, facilitating the accumulation of air pollutants and contributing to the high pollutants level in the afternoon. Pollutants formed in the afternoon are transported by the valley breeze from the urban to the mountain area, serving as a pollutant reservoir to elevate the background pollutants level in the morning when delivered back to the urban area by the mountain breeze.

Fig. 3c and d shows the evolution of the vertical profiles of the hourly horizontal winds observed by the radar wind profiler at Baodi in Tianjin on August 9 and 10. On August 9, there is a clear wind shift from the northwest to southwest during 11:00–14:00 BJT, showing the impact of the land-sea breeze. During the transition period, the wind speed decreases considerably. On August 10, between 08:00–11:00 BJT, the horizontal winds become weak and disordered. After 12:00 BJT, the sea breeze commences to develop and intensify, with the wind direction changing from southwesterly to southeasterly. It is worth noting that the difference in the simulated and observed wind direction is noticeable on August 9

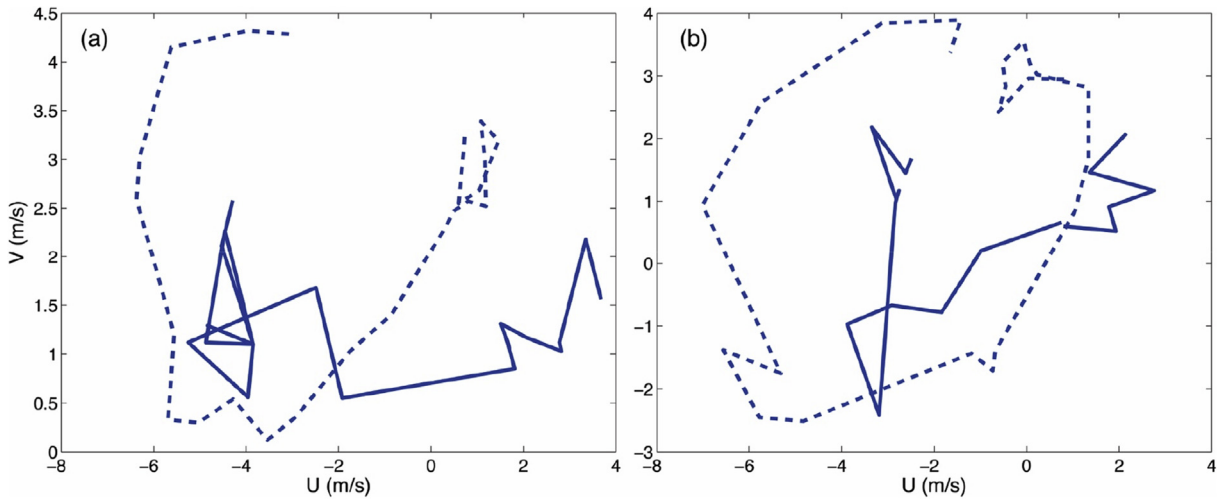

Fig. 2. The simulated (blue dashed line) and observed (blue solid line) wind hodographs at the sites located at (a) 117.71°E, 38.46°N and (b) 118.05°E, 38.04°N on August 10, 2013. (For interpretation of the references to colour in this figure legend, the reader is referred to the web version of this article.)

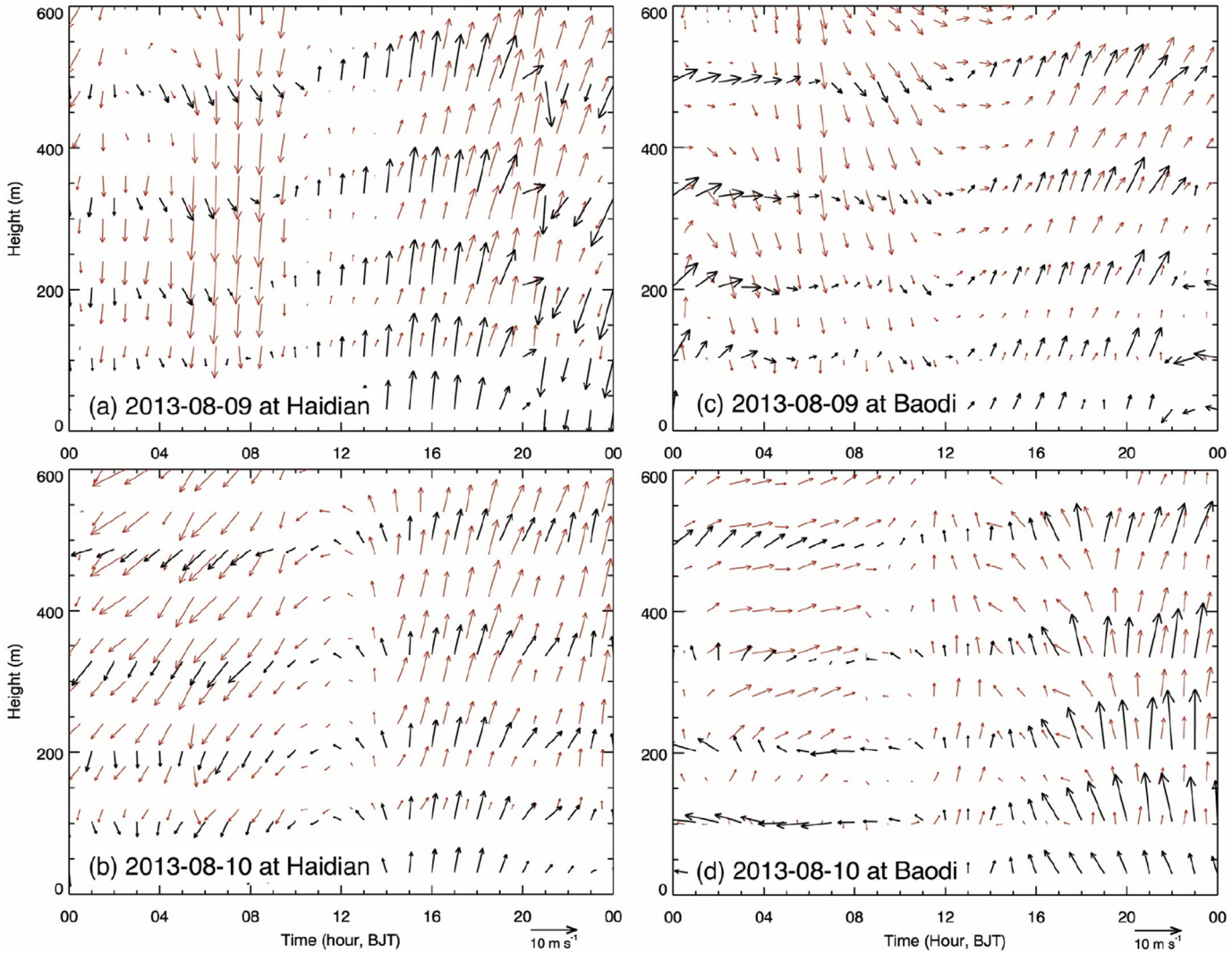

Fig. 3. Temporal variations of simulated (black arrows) and wind profiler observed (red arrows) horizontal winds at Haidian in Beijing on August (a) 9 and (b) 10, 2013 and at Baodi in Tianjin on August (c) 9 and (d) 10, 2013. (For interpretation of the references to colour in this figure legend, the reader is referred to the web version of this article.)

(Fig. 3c). The uncertainties in temperature and wind fields simulations might constitute the main reason for the discrepancy. Furthermore, although the experience with land-sea breeze simulations has extended over many decades, it is still difficult for current numerical weather prediction models, even in research mode, to reproduce the location, timing, depth, and intensity of sea-breeze front (Banta et al., 2005). Generally, the model reasonable reproduces the sea breeze formation compared to the observation.

3.2. Impacts of the local circulations on the air pollution

Fig. 4 presents the diurnal profiles of observed and simulated near-surface $PM_{2.5}$, O_3, NO_2, and CO concentrations averaged over monitoring stations in BTH from 9 to 11 August 2013. The mean bias (*MB*), the root mean square error (*RMSE*), and the index of agreement (*IOA*) are used to evaluate the WRF-CHEM model simulations of the air pollutants.

$$MB = \frac{1}{N}\sum_{i=1}^{N}(P_i - O_i) \tag{1}$$

$$RMSE = \left[\frac{1}{N}\sum_{i=1}^{N}(P_i - O_i)^2\right]^{\frac{1}{2}} \tag{2}$$

$$IOA = 1 - \frac{\sum_{i=1}^{N}(P_i - O_i)^2}{\sum_{i=1}^{N}\left(|P_i - \overline{O}| + |O_i - \overline{O}|\right)^2} \tag{3}$$

where P_i and O_i are the simulated and observed variables, respectively. N is the total number of the predictions used for comparisons, and $\overline{O}$ denotes the average of the observation. *IOA* ranges from 0 to 1, with 1 indicating perfect agreement between model and observation.

The WRF-CHEM model performs reasonably well in reproducing the $PM_{2.5}$ variations compared to observations in BTH. The *MB* and *RMSE* are -1.9 μg m^{-3} and 24.1 μg m^{-3}, respectively, and the *IOA* is 0.85. The model well predicts the temporal variations of O_3 concentrations, with an *IOA* of 0.96. On August 9, the model considerably underestimates the O_3 concentrations in the afternoon, but the agreement between modeled and observed O_3 is better than that for $PM_{2.5}$ and NO_2. The model also reasonably produces the NO_2 diurnal variations, but is subject to overestimate the NO_2 concentrations during nighttime, which might be due to the biased

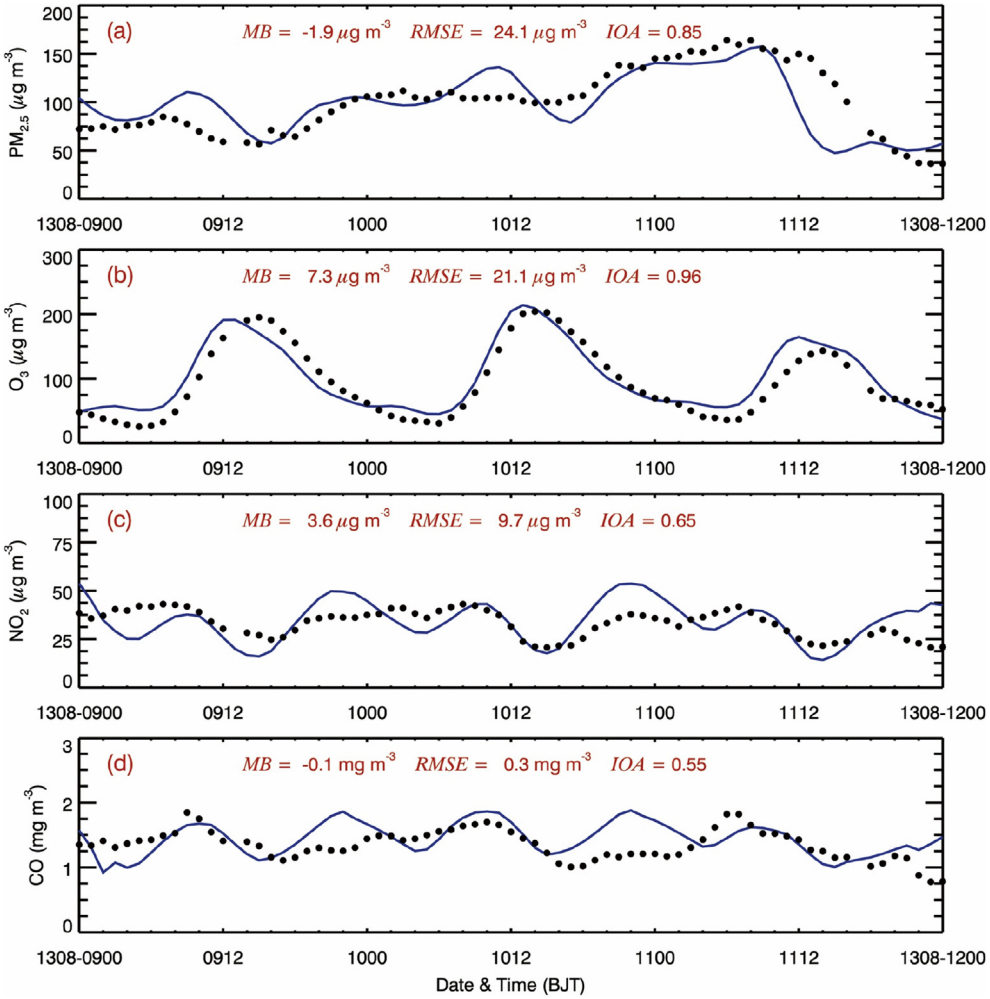

Fig. 4. Comparison of measured (black dots) and predicted (blue line) diurnal profiles of near-surface hourly (a) $PM_{2.5}$, (b) O_3, (c) NO_2, and (d) CO concentrations averaged over all ambient monitoring stations in BTH from 9 to 11 August 2013. (For interpretation of the references to colour in this figure legend, the reader is referred to the web version of this article.)

PBL simulations, the complex NO_x chemistry, or uncertainties of emissions. In addition, the nighttime CO overestimation is not as substantial as those of NO_2, showing that the complex NO_x chemistry or uncertainties of NO_x emissions might constitutes the main reason for the nighttime NO_2 overestimation, considering that CO is generally regarded as a tracer. Figs. S4 and S5 provide the diurnal profiles of observed and simulated near-surface $PM_{2.5}$, O_3, NO_2, and CO concentrations from 9 to 11 August 2013 at two monitoring sites in Beijing and Tianjin, respectively. The observed NO_2 and CO fluctuate considerably during the episode, and frequently reach their peaks during nighttime or in the early morning, which is partially caused by the low PBL height. In general, the model reasonably yields the observed variations of the pollutants, but the model biases are rather large, particularly for the NO_2 simulations.

The evolution of the simulated and observed surface O_3 distributions during the episode along with the simulated surface wind fields is presented in Fig. 5. The simulated variations of the O_3 spatial patterns are generally in good agreement with the observations at the ambient monitoring sites in BTH. On August 9 (Fig. 5a), during the nighttime (02:00 BJT), the simulated O_3 concentration over the land is low because of titration from NO_x emissions and the inactive photochemical process due to lack of sunlight. The maximum O_3 level is located over the Bohai Gulf, which is caused by the high O_3 formation during daytime over the gulf from O_3 precursors transported from the land by the offshore sea breeze and lack of NO_x emissions. At 12:00 BJT, the wind along the coastline becomes nearly calm or weak, which is favorable for the accumulations of the pollutant emissions. In the afternoon (Fig. 5c), the onshore sea breeze starts to develop, which can convey the high O_3 formed over the gulf to the land. Additionally, the sea breeze causes the formation of a convergence zone along the seaside, on one hand possibly facilitating the pollutant accumulation to result in the severe air pollution, on the other hand inducing convections to loft pollutants outside of PBL to decrease the pollutants level. Along with the increase of the onshore sea breeze, the maximum O_3 concentration generally occurs around 14:00–15:00 BJT in BTH. In the evening, the offshore breeze becomes dominant wind, delivering the pollutants to the Bohai Gulf again. The O_3 evolution pattern on August 10 is similar to that on August 9 except that the O_3 concentration on August 10 is higher, showing the accumulation effect contributed by the local circulations.

Fig. 6 shows the spatial distributions of the simulated and

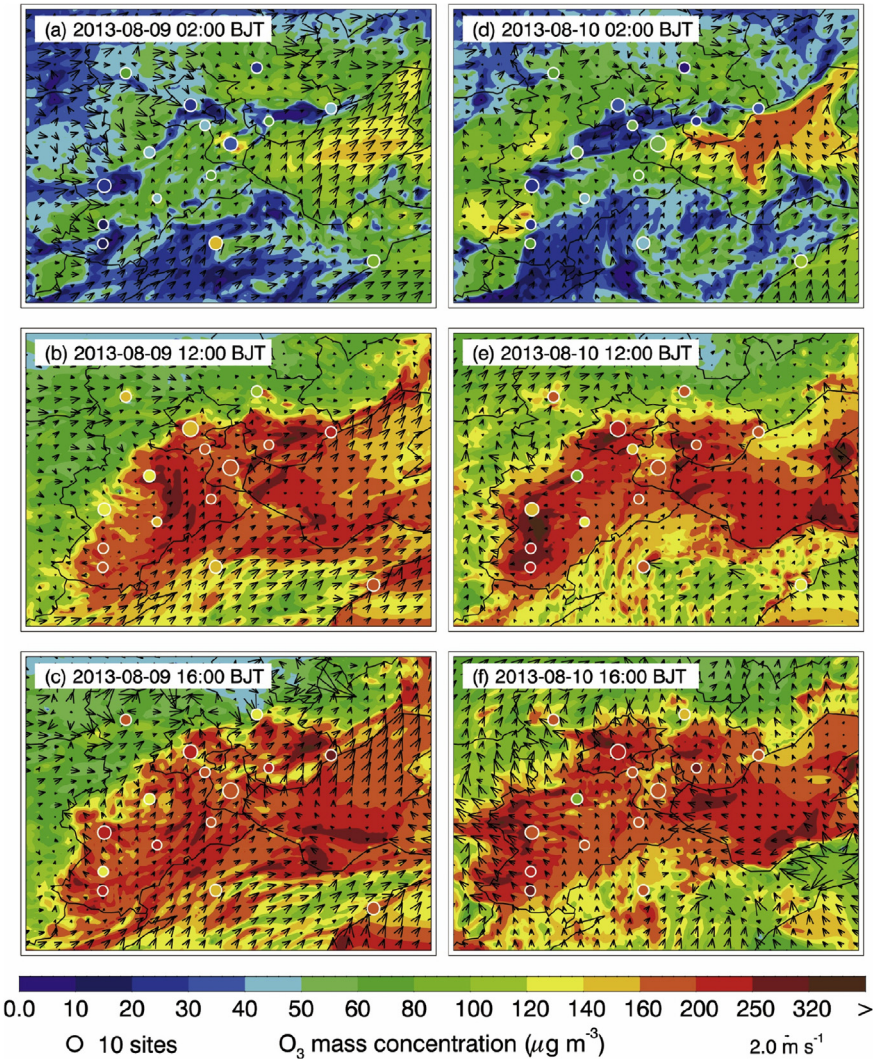

Fig. 5. Pattern comparison of simulated vs. observed near-surface O_3 concentrations at (a) 02:00, (b) 12:00, and (c) 16:00 BJT on August 9, and (d) 02:00, (e) 12:00, and (f) 16:00 BJT on August 10, 2013. Colored circles: O_3 observations; color contour: O_3 simulations; black arrows: simulated surface winds. (For interpretation of the references to colour in this figure legend, the reader is referred to the web version of this article.)

observed $PM_{2.5}$ mass concentrations during the episode along with the simulated surface winds. The simulated $PM_{2.5}$ spatial patterns are generally consistent well with the observations at the ambient monitoring sites in BTH, but the biases of $PM_{2.5}$ simulations during nighttime are still considerably large. In the early morning on August 9, due to the accumulated emissions and residual pollutants from the previous day as well as the low PBL height, the $PM_{2.5}$ concentrations are high in the plain area of BTH. The offshore land breeze also gradually develops and transports the pollutants formed in Shandong province to the Bohai Gulf. In the afternoon, the $PM_{2.5}$ level in BTH is decreased caused by the enhanced vertical dispersion due to the PBL development. However, the $PM_{2.5}$ level over the gulf is still high because of the low PBL height and the formed high O_3 concentrations enhancing the formation of secondary aerosols. The increasing onshore breeze transports the $PM_{2.5}$ over the gulf to the land area, contributing the $PM_{2.5}$ to Tianjin and other cities in the coastal area in the afternoon and evening. In the early morning on August 10, the development of the offshore sea breeze brings pollutants in Shandong province to the gulf again. In the afternoon and evening, the $PM_{2.5}$ over the gulf are delivered to Tianjin by the onshore sea breeze and even affect the air quality in Beijing.

Fig. 7 depicts the cross-sections of the simulated wind vectors, $PM_{2.5}$ concentrations, and the PBL height on August 9 and 10 along the cross line indicated in Fig. 1b, which is almost perpendicular to the coastline of the Bohai Gulf. In the morning on August 9, at 08:00 BJT (Fig. 7a), the PBL height is low both over the land (several hundred meters) and sea (around one hundred meters), leading to the relatively high pollutants level in the low level atmosphere. The offshore land breeze near the coastline and the downward mountain breeze close to the mountain area are both clear in the vertical layer of near 300–400 m. In the afternoon, at 16:00 BJT (Fig. 7b), the PBL height is substantially increased, with the maximum of around 2.0 km over the land, and the surface level $PM_{2.5}$ concentrations are decreased due to efficient dispersion of pollutants in the PBL. The strong onshore sea breeze causes the formation of a convergence zone near the coastline, inducing the upward movement to transport the $PM_{2.5}$ to the high level atmosphere. The valley breeze also delivers the $PM_{2.5}$ to the mountain area. At 21:00 BJT (Fig. 7c), due to cooling of the mountain areas, the downward mountain breeze transports the $PM_{2.5}$ toward the gulf, and the convergence zone is formed when the onshore sea breeze meets the mountain breeze, facilitating the $PM_{2.5}$ to disperse in the vertical direction. The cross-sections on August 10 are generally similar to that on August 9, but the offshore land breeze and the upward valley breeze in the morning are stronger than that on August 9.

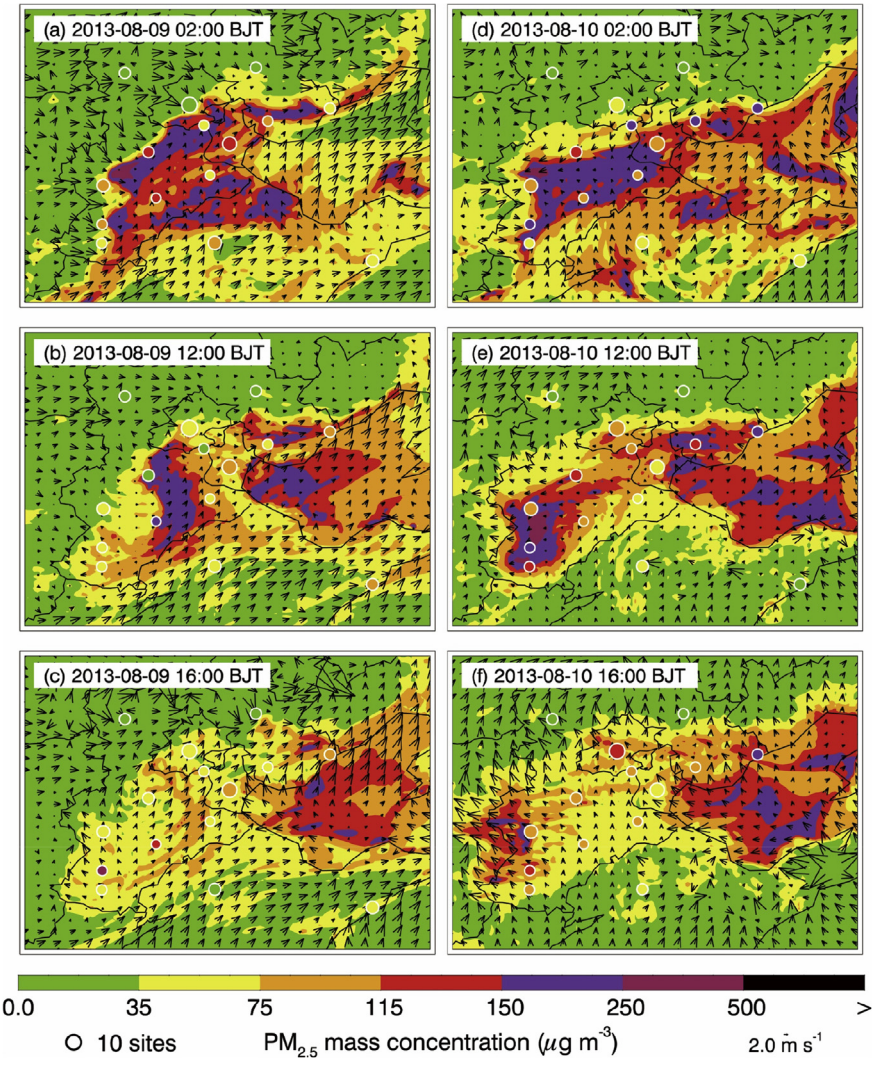

Fig. 6. Same as Fig. 5, but for $PM_{2.5}$.

Apparently, more pollutants are transported to the mountain area by the valley breeze on August 10. In addition, the onshore sea breeze in the afternoon and evening is also intensified on August 10 compared to August 9, even intruding to the foothill of the mountains, but the downward mountain breeze is weak, causing the higher $PM_{2.5}$ level in Beijing.

4. Summary and discussions

In the present study, observational analyses and numerical model simulations are utilized to investigate the impact of sea-land breeze and mountain valley breeze circulations on a high-pollution event occurred in BTH during August 9–11, 2013. The analysis of the large-scale meteorological conditions over BTH has shown that BTH is influenced by the subtropical high in the southeast and the low in the northeast at 850 hPa on August 9 and 10, indicating that BTH is under the control of the relatively weak westerly flow on these two days. The surface wind observations along with simulations and the measurements of two radar wind profilers in BTH have also clearly demonstrated the development of the local circulations during

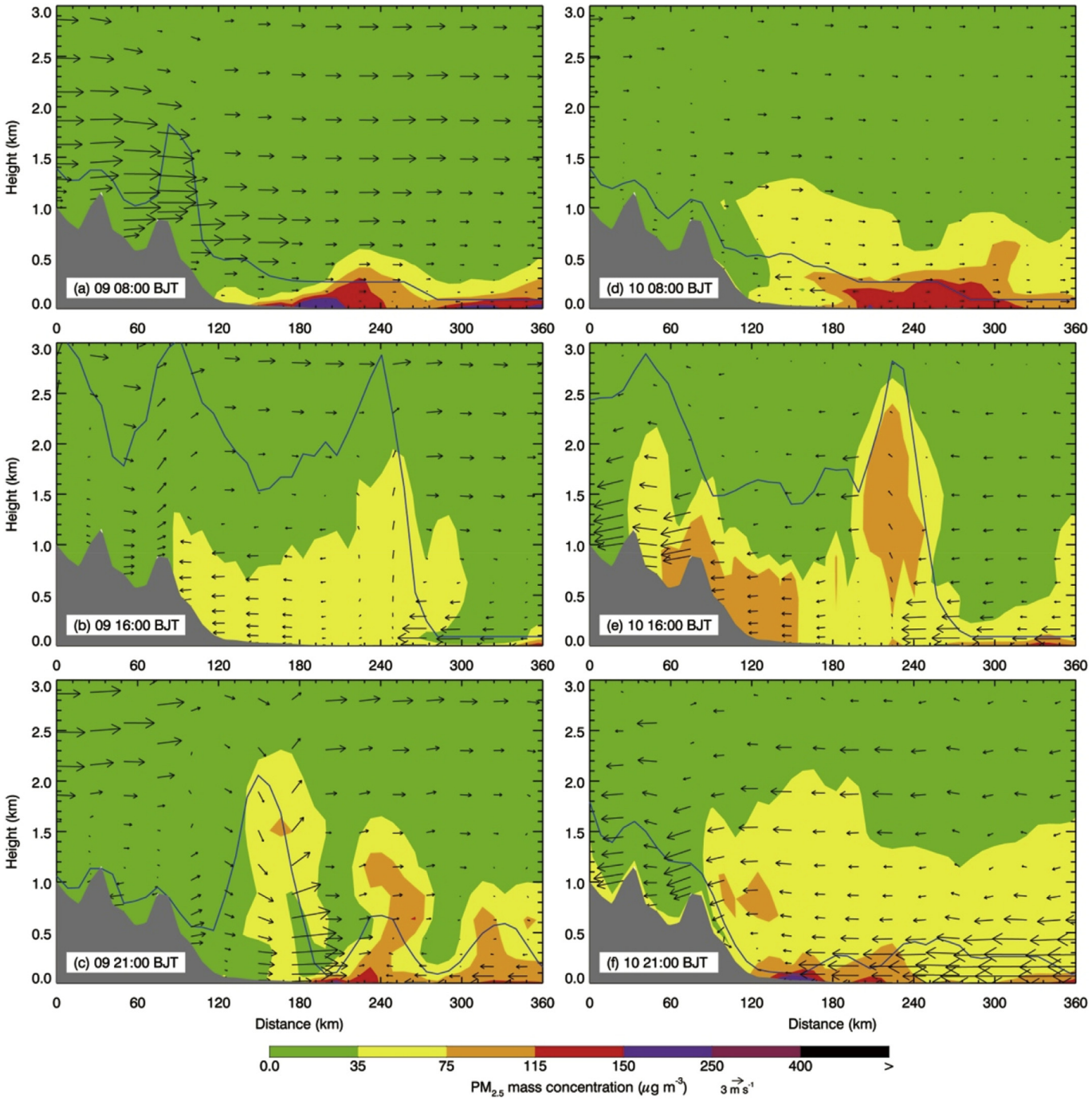

Fig. 7. Vertical distributions of $PM_{2.5}$ concentrations along the cross line in Fig. 1 at (a) 08:00, (b) 16:00, and (c) 21:00 BJT on August 9, 2013, and (d) 08:00, (e) 16:00, and (f) 21:00 BJT on August 10, 2013. Color contour: $PM_{2.5}$ simulations; black arrows: simulated winds; blue line: PBL height. (For interpretation of the references to colour in this figure legend, the reader is referred to the web version of this article.)

these two days, including the mountain-valley breeze circulation in Beijing and the sea-land breeze circulation along the coast area of the Bohai Gulf. The development of the local circulations not only facilitates the accumulation of pollutants to deteriorate the air quality during the wind transition, also causes the formation of a convergence zone to induce upward movement, mitigating the surface pollution to some degree.

The WRF-CHEM model generally performs well in simulating the observed pollution event. The model reasonably well reproduces the evolution of the observed surface winds. The predicted temporal variations and spatial distributions of $PM_{2.5}$ and O_3 concentrations are in good agreement with observations in BTH. The model has also successfully simulated the development of the mountain-valley breeze circulation in Beijing and the sea-land breeze circulation along the coastal area of the Bohai Gulf. The upward valley breeze and the offshore land breeze prevail in the morning while the downward mountain breeze and the onshore sea breeze start to take over in the afternoon.

In the morning, the offshore land breeze transports the pollutants formed in Shandong province to the Bohai Gulf and high O_3 and $PM_{2.5}$ concentrations are formed over the gulf due to accumulation of their precursors in case of the low PBL height. In the afternoon and evening, the onshore sea breeze delivers the pollutants to the coastal area, where the air quality is generally deteriorated when the sea breeze front passes over. The intensified sea breeze even transports the pollutants to affect the air quality in Beijing. The upward valley breeze brings the pollutants in the urban area of Beijing to the mountain area in the afternoon, and the downward mountain breeze transports the pollutants back. However, compared to the land-sea breeze circulation, the intensity of the mountain-valley breeze circulation is weak.

In general, the pollution event occurred during August 9–10 is the combination result of the local emission and the meteorological conditions at both large and local scales. The local circulations usually play an important role when the large-scale meteorological conditions are relatively weak.

It is worth noting that the most severe air pollution events generally occur during wintertime in BTH when the southerly wind is prevalent. The downward mountain breeze is subject to alleviate the air pollution in the foothills of Taihang Mountains and the Yanshan Mountains to some degree.

Acknowledgements

Naifang Bei is supported by the National Natural Science Foundation of China (No. 41275101 and No. 41430424) and the Fundamental Research Funds for the Central Universities of China. Guohui Li is supported by “Hundred Talents Program” of the Chinese Academy of Sciences and the National Natural Science Foundation of China (No. 41661144020). This work is financially supported by National Key R&D Plan (Quantitative Relationship and Regulation Principle between Regional Oxidation Capacity of Atmospheric and Air Quality (2017YFC0210000)).

Appendix A. Supplementary data

Supplementary data related to this article can be found at https://doi.org/10.1016/j.envpol.2017.11.066.

References

Banta, R.M., Senff, C.J., Ryerson, T.B., Nielsen-Gammon, J.W., Darby, L.S., Alvarez, R.J., Sandberg, S.P., Williams, E.J., Trainer, M., 2005. A bad air day in Houston. Bull. Am. Meteorol. Soc. 86, 657–669.

Bao, J.W., Michelson, S.A., McKeen, S.A., Grell, G.A., 2005. Meteorological evaluation of a weather-chemistry forecasting model using observations from the TEXAS AQS 2000 field experiment. J. Geophys. Res. 110, D21105. https://doi.org/10.1029/2004JD005024.

Bei, N., de Foy, B., Lei, W., Zavala, M., Molina, L.T., 2008. Using 3DVAR data assimilation system to improve ozone simulations in the Mexico City Basin. Atmos. Chem. Phys. 8, 7353–7366.

Bei, N., Lei, W., Zavala, M., Molina, L.T., 2010. Ozone predictabilities due to meteorological uncertainties in Mexico City Basin using ensemble forecasts. Atmos. Chem. Phys. 10, 6295–6309.

Bei, N., Li, G., Zavala, M., Barrera, H., Torres, R., Grutter, M., Gutiérrez, W., García, M., Ruiz-Suarez, L.G., Ortinez, A., Guitierrez, Y., Alvarado, C., Flores, I., Molina, L.T., 2013. Meteorological overview and plume transport patterns during Cal-Mex 2010. Atmos. Environ. 70, 477–489.

Bei, N., Li, G., Huang, R., Cao, J., Meng, N., Feng, T., Liu, S., Zhang, T., Zhang, Q., Molina, L.T., 2016a. Typical synoptic situations and their impacts on the wintertime air pollution in the Guanzhong Basin, China. Atmos. Chem. Phys. 16, 7373–7387.

Bei, N., Xiao, B., Meng, N., Feng, T., 2016b. Critical role of meteorological conditions in a persistent haze episode in the Guanzhong Basin, China. Sci. Total Environ. 550, 273–284.

Chan, C.K., Yao, X., 2008. Air pollution in mega cities in China. Atmos. Environ. 42, 1–42.

Chan, L.Y., Chan, C.Y., Qin, Y., 1998. Surface ozone pattern in Hong Kong. J. Appl. Meteorol. 37, 1153–1165.

Chen, Z., Cheng, S., Li, J., Guo, X., Wang, W., Chen, D., 2008. Relationship between atmospheric pollution processes and synoptic pressure patterns in Northern China. Atmos. Environ. 42, 6078–6087.

Chen, F., Dudhia, J., 2001. Coupling an advanced land surface-hydrology model with the Penn State-NCAR MM5 modeling system. Part I: model implementation and sensitivity. Mon. Weather Rev. 129, 569–585. https://doi.org/10.1175/1520-0493(2001)129<0569:caalsh>2.0.co;2.

Chou, M.D., Suarez, M.J., 1999. A solar radiation parameterization for atmospheric studies. NASA Tech. Rep. 15, 38. NASA/TM-1999–10460.

Chou, M.D., Suarez, M.J., 2001. A thermal infrared radiation parameterization for atmospheric studies. NASA Tech. Rep. 19, 55. NASA/TM-2001–104606.

Ding, A.J., Wang, T., Zhao, M., Wang, T.J., Li, Z.K., 2004. Simulation of sea-land breezes and a discussion of their implications on the transport of air pollution during a multiday ozone episode in the Pearl River Delta of China. Atmos. Environ. 38, 6737–6750. https://doi.org/10.1016/j.atmosenv.2004.09.017.

Fan, S.J., Dong, J., Guo, L.L., Wang, A.Y., Somg, L.L., Liu, A.J., Xie, J.W., 2006. Analysis of the impact of urban growth on the temperature field in Guangzhou. J. Trop. Meteorol. 12, 24–28.

Fang, M., Chan, C.K., Yao, X.H., 2009. Managing air quality in a rapidly developing nation: China. Atmos. Environ. 43, 79–86.

Fast, J.D., Gustafson, W.I., Easter, R.C., Zaveri, R.A., Barnard, J.C., Chapman, E.G., Grell, G.A., Peckham, S.E., 2006. Evaluation of ozone, particulates, and aerosol direct radiative forcing in the vincity of Houston using a fully-coupled meteorology-chemistry-aerosol model. J. Geophys. Res. 111 https://doi.org/10.1029/2005JD006721.

Feng, T., Bei, N., Huang, R., Cao, J., Zhang, Q., Zhou, W., Tie, X., Liu, S., Zhang, T., Su, X., Lei, W., Molina, L.T., Li, G., 2016. Summertime ozone formation in Xi'an and surrounding areas, China. Atmos. Chem. Phys. 16, 4323–4342. https://doi.org/10.5194/acp-16-4323-2016.

Gao, Y., Liu, X., Zhao, C., Zhang, M., 2011. Emission controls versus meteorological conditions in determining aerosol concentrations in Beijing during the 2008 Olympic Games. Atmos. Chem. Phys. 11, 12437–12451. https://doi.org/10.5194/acp-11-12437-2011.

Grell, G.A., Devenyi, D., 2002. A generalized approach to parameterizing convection combining ensemble and data assimilation techniques. Geophys. Res. Lett. 29 (14) https://doi.org/10.1029/2002GL015311.

Grell, G.A., Peckham, S.E., Schmitz, R., McKeen, S.A., Wilczak, J., Eder, B., 2005. Fully coupled “online” chemistry within the WRF model. Atmos. Environ. 39, 6957–6975.

Guenther, A., Karl, T., Harley, P., Wiedinmyer, C., Palmer, P.I., Geron, C., 2006. Estimates of global terrestrial isoprene emissions using MEGAN (Model of Emissions of Gases and Aerosols from Nature). Atmos. Chem. Phys. 6, 3181–3210.

Hong, S.Y., Lim, J.O.J., 2006. The WRF single-moment 6-class microphysics scheme (WSM6). Asia-Pac. J. Atmos. Sci. 42, 129–151.

Horowitz, L.W., Walters, S., Mauzerall, D.L., Emmons, L.K., Rasch, P.J., Granier, C., Tie, X.X., Lamarque, J.F., Schultz, M.G., Tyndall, G.S., Orlando, J.J., Brasseur, G.P., 2003. A global simulation of tropospheric ozone and related tracers: description and evaluation of MOZART, version 2. J. Geophys. Res. Atmos. 108 (29) https://doi.org/10.1029/2002jd002853.

Janjić, Z.I., 2002. Nonsingular Implementation of the Mellor-Yamada Level 2.5 Scheme in the NCEP Meso Model. Ncep Office Note, p. 436.

Li, G., Lei, W., Zavala, M., Volkamer, R., Dusanter, S., Stevens, P., Molina, L.T., 2010. Impacts of HONO sources on the photochemistry in Mexico City during the MCMA-2006/MILAGO Campaign. Atmos. Chem. Phys. 10, 6551–6567.

Li, G., Bei, N., Cao, J., Wu, J., Long, X., Feng, T., Dai, W., Liu, S., Zhang, Q., Tie, X., 2017a. Widespread and persistent ozone pollution in eastern China during the non-winter season of 2015: observations and source attributions. Atmos. Chem. Phys. 17, 2759–2774. https://doi.org/10.5194/acp-17-2759-2017.

Li, G., Bei, N., Cao, J., Huang, R., Wu, J., Feng, T., Wang, Y., Liu, S., Zhang, Q., Tie, X., Molina, L.T., 2017b. A possible pathway for rapid growth of sulfate during haze days in China. Atmos. Chem. Phys. 17, 3301–3316.

Liu, H., Chan, C.L., 2002. An investigation of air-pollutant patterns under sea-land

breezes during a severe air-pollution episode in Hong Kong. Atmos. Environ. 36, 591–601.
Long, X., Tie, X., Cao, J., Huang, J., Feng, T., Li, N., Zhao, S., Tian, J., Li, G., Zhang, Q., 2016. Impact of crop field burning and mountains on heavy haze in the North China Plain: a case study. Atmos. Chem. Phys. 16, 9675–9691. https://doi.org/10.5194/acp-16-9675-2016.
Miao, Y., Liu, S., Zheng, Y., et al., 2015. Numerical study of the effects of local atmospheric circulations on a pollution event over Beijing-Tianjin-Hebei, China. J. Environ. Sci. 30, 9–20.
Parrish, D., Zhu, T., 2009. Clean air for megacities. Science 326, 674–675.
Philipp, A., Bartholy, J., Beck, C., Erpicum, M., Esteban, P., Fettweis, X., Huth, R., James, P., Jourdain, S., Kreienkamp, F., 2010. COST733CAT-a database of weather and circulation type classifications. Phys. Chem. Earth 35, 360–373.
Pope III, C.A., Dockery, D.W., 2006. Health effects of fine particulate air pollution: lines that connect. J. Air Waste Manage. 56, 709–742.
Tie, X.X., Wu, D., Brasseur, G., 2009. Lung cancer mortality and exposure to atmospheric aerosol particles in Guangzhou, China. Atmos. Environ. 43 (14), 2375–2377.
Tie, X., Zhang, Q., He, H., Cao, J., Han, S., Gao, Y., Li, X., Jia, X., 2015. A budget analysis on the formation of haze in Beijing. Atmos. Environ. 100, 25–36.
Wang, T., Lam, K.S., Lee, A.S.Y., Pang, S.W., Tsui, W.S., 1998. Meteorological and chemical characteristics of the photochemical ozone episodes observed at Cape D'Aguilar in Hong Kong. J. Appl. Meteorol. 37, 1167–1178.
Wang, M., Zhu, T., Zheng, J., Zhang, R.Y., Zhang, S.Q., Xie, X.X., Han, Y.Q., Li, Y., 2009. Use of a mobile laboratory to evaluate changes in on-road air pollutants during the Beijing 2008 Summer Olympics. Atmos. Chem. Phys. 9, 8247–8263. https://doi.org/10.5194/acp-9-8247-2009.
Wang, M., Zhu, T., Zhang, J.P., Zhang, Q.H., Lin, W.W., Li, Y., Wang, Z.F., 2011. Using a mobile laboratory to characterize the distribution and transport of sulfur dioxide in and around Beijing. Atmos. Chem. Phys. 11, 11631–11645. https://doi.org/10.5194/acp-11-11631-2011.
Wang, S., Zhao, M., Xing, J., Wu, Y., Zhou, Y., Lei, Y., He, K., Fu, L., Hao, J., 2010. Quantifying the air pollutants emission reduction during the 2008 Olympic Games in Beijing. Environ. Sci. Technol. 44, 2490–2496.
Wu, J., Li, G., Cao, J., Bei, N., Wang, Y., Feng, T., Huang, R., Liu, S., Zhang, Q., Tie, X., 2017. Contributions of trans-boundary transport to summertime air quality in Beijing, China. Atmos. Chem. Phys. 17, 2035–2051. https://doi.org/10.5194/acp-17-2035-2017.
Zhang, F., Bei, N., Nielsen-Gammon, J.W., Li, G., Zhang, R., Stuart, A.L., 2007. Impacts of meteorological uncertainties on ozone pollution predictability estimated through meteorological and photochemical ensemble forecasts. J. Geophys. Res. 112, 195–205.
Zhang, J., Mauzerall, D.L., Zhu, T., Liang, S., Ezzati, M., Remais, J.V., 2010a. Environmental health in China: progress towards clean air and safe water. Lancet 375, 1110–1119.
Zhang, J.P., Zhu, T., Zhang, Q.H., Li, C.C., Shu, H.L., Ying, Y., Dai, Z.P., Wang, X., Liu, X.Y., Liang, A.M., Shen, H.X., Yi, B.Q., 2012. The impact of circulation patterns on regional transport pathways and air quality over Beijing and its surroundings. Atmos. Chem. Phys. 12, 5031–5053. https://doi.org/10.5194/acp-12-5031-2012.
Zhang, Q.H., Zhang, J.P., Xue, H.W., 2010b. The challenge of improving visibility in Beijing. Atmos. Chem. Phys. 10, 7821–7827. https://doi.org/10.5194/acp-10-7821-2010.
Zhang, X., Wang, Y., Lin, W., Zhang, Y., Zhang, X., Zhao, P., Yang, Y., Wang, J., Hou, Q., Che, H., 2009. Changes of atmospheric composition and optical properties over BEIJING-2008 Olympic monitoring campaign. B. Am. Meteorol. Soc. 90, 1633–1651.
Zhao, S., Tie, X., Cao, J., Zhang, Q., 2015. Impacts of mountains on black carbon aerosol under different synoptic meteorology conditions in the Guanzhong region, China. Atmos. Res. 164–165 (1), 286–296.